Korean J. Chem. Eng., 32(7), 1278-1288 (2015)
DOI: 10.1007/s11814-014-0311-0

pISSN: 0256-1115
eISSN: 1975-7220

The effect of preparation factors on the structural and catalytic properties of mesoporous nanocrystalline iron-based catalysts for high temperature water gas shift reaction

Fereshteh Meshkani* and Mehran Rezaei*,,†**

*Catalyst and Advanced Materials Research Laboratory, Chemical Engineering Department, Faculty of Engineering, University of Kashan, Kashan, Iran
**Institute of Nanoscience and Nanotechnology, University of Kashan, Kashan, Iran
(*Received 22 August 2014 • accepted 15 October 2014*)

Abstract−A systematic study was done on the effect of preparation factors on the structural and catalytic properties of mesoporous nanocrystalline iron-based catalysts in high temperature water gas shift reaction. The catalysts were prepared by coprecipitation method, and the effect of the main preparation factors (pH, refluxing temperature, refluxing time, concentration of the precursors solution) was studied. The catalysts were characterized by powder X-ray diffraction (XRD), N_2 adsorption (BET), Temperature programmed reduction (TPR), transmission and scanning electron microscopies (TEM, SEM) techniques. The results revealed that the preparation factors affected the textural and catalytic properties of the Fe-Cr-Cu catalyst. The results showed that the prepared catalyst with the highest activity showed higher specific surface area compared to commercial catalyst and consequently exhibited higher activity in high temperature water gas shift reaction. The TEM analysis showed a nanostructure for this sample with crystallite size less than 20 nm.

Keywords: Coprecipitation, Iron Based, Water-gas Shift, Nanostructure

INTRODUCTION

The water gas shift reaction is moderately exothermic and limited by its thermodynamic equilibrium [1]. Owing to thermodynamic limitations and its exothermicity, the reaction is divided into two steps on the industrial scale: high temperature and low temperature water gas shift reactions [2,3]. The high temperature water gas shift reaction is usually performed between 375 and 450 °C, and the low temperature water gas shift operates between 200 and 300 °C [4,5]. Depending on the feed composition, the carbon monoxide concentration of the high temperature water gas shift product ranges between 2 and 3 vol%, whereas the low temperature water gas shift product contains between 0.05-1 vol% [6]. The chromia promoted iron oxide is the conventional catalyst for the high temperature water gas shift (WGS) reaction for the production of hydrogen in industry [7]. It is known that the magnetite (Fe_3O_4) phase is the active phase in high temperature water gas shift catalysts. The commercial lifetime of pure magnetite catalysts is limited because of thermal sintering and chromium oxide addition;, 8-12 wt% Cr_2O_3, has been found to stabilize the surface area and extend the catalyst life to 2-5 years. Cr^{+3} exists in solid solution within the Fe_3O_4 phase as an inverse spinel lattice and discrete Cr_2O_3 grains are not detected. In addition, commercial catalysts include 2-4 wt% CuO as a promoter, which may provide active sites via formation of additional active sites [8,9].

The preparation factors of catalyst synthesis method have a significant effect on the structural properties of the prepared catalysts. Coprecipitation is the most conventional method in preparation of mixed oxide catalysts. In this method there are several parameters, such as concentration of the solution precursors, pH, refluxing temperature, refluxing time, which can affect the structural and activity properties of the final catalysts [10]. Concerning iron oxides, several works have been carried out to state the effect of the preparation method on the properties of these catalysts [11]. We did a systematic study to investigate the effect of preparation factors on the structural and catalytic properties of Fe-Cr-Cu catalyst in high temperature water gas shift reaction.

EXPERIMENTAL

1. Materials

The starting materials were the divalent ($FeSO_4 \cdot 7H_2O$) and trivalent ($Fe(NO_3)_3 \cdot 9H_2O$) iron salts as iron precursors. Chromium (III) nitrate nonahydrate ($Cr(NO_3)_3 \cdot 9H_2O$) and copper (II) nitrate trihydrate ($Cu(NO_3)_2 \cdot 3H_2O$) and NaOH were also used as Cr and Cu precursors and precipitation agent, respectively. All reagents were used as received without further purification or additional treatment.

2. Catalyst Preparation

Fe-Cr-Cu catalysts containing 88.8 wt% Fe_2O_3, 8.88 wt% of Cr_2O_3 and 2.32 wt% of CuO were prepared by coprecipitation method. Initially, based on the catalyst composition an aqueous solution of the $FeSO_4 \cdot 7H_2O$ and $Fe(NO_3)_3 \cdot 9H_2O$, $Cr(NO_3)_3 \cdot 9H_2O$ and $Cu(NO_3)_2 \cdot 3H_2O$ was prepared, deoxygenated by continuously bubbling argon

†To whom correspondence should be addressed.
E-mail: rezaei@kashanu.ac.ir

gas through the reaction solution. The Fe^{2+} : Fe^{3+} ratio was chosen as 1 : 2. After that NaOH solution (1 M) was added dropwise to adjust the desired pH value. After precipitation, the suspension was refluxed at different temperatures for a certain time under continuous stirring. Then the suspension was filtered and washed with hot deionized water for effective removal of ions. The final product was dried at 90 °C for 24 h and calcined at different temperatures for 4 h in air atmosphere.

3. Characterization

The specific surface area was evaluated by the BET method using N_2 adsorption at −196 °C with an automated gas adsorption analyzer (Tristar 3020, Micromeritics). The Barrett, Joyner and Halenda (BJH) method was used to determine the pore size distribution from the desorption branch of the isotherm. Temperature-programmed reduction (TPR) was carried out using an automatic apparatus (Chemisorb 2750, Micromeritics) equipped with a thermal conductivity detector. Before the TPR experiment, a fresh sample (ca. 50 mg) was treated under an inert atmosphere at 250 °C for 2 h, and then subjected to a reduction treatment with a heating rate of 10 °C/min in a reducing gas flow (20 mL/min) containing a mixture of H_2 : Ar (10 : 90). The crystalline structure of the prepared catalysts was determined by X-ray powder diffraction (XRD) using a X-ray diffractometer (PANalytical X'Pert-Pro) using a Cu-Kα monochromatized radiation source and a Ni filter. The surface morphology of the catalysts was observed with transmission electron microscope (JEOL JEM-2100UHR).

4. Catalytic Reaction

The high temperature water gas shift reaction tests were performed in a quartz tubular fixed bed flow reactor (i.d. 8 mm) under atmospheric pressure. A thermocouple was inserted in the bottom of the catalyst bed to measure the reaction temperature. The total catalyst charged for each reaction was held constant (100 mg and with particle size of 0.25-0.5 mm). A gaseous mixture of 30% CO, 60% H_2, 10% CO_2 and a water steam with desired H_2O/dry gas molar ratio were supplied to the catalyst bed. The gas flow rates were controlled by the mass flow controllers (BROOKS 5850) and water flow rates by a programmable syringe pump.

Prior to reaction, the catalysts were reduced using a gaseous mixture of 30% CO, 60% H_2, 10% CO_2 and a water steam with a H_2O/dry gas molar ratio of 0.6 at 400 °C for 2 h. The activity tests were carried out at different temperatures ranging from 300 °C to 500 °C in steps of 50 °C. Before each analysis, the effluent was passed through a water-trap to remove the water from the product stream. The gas composition was analyzed by an HID YL-6100 gas chromatograph equipped with a carboxen1010 column.

RESULTS AND DISCUSSION

The pore size distributions of the prepared catalysts under different pH values are shown in Fig. 1(a). Increasing in pH value shifted the pore size distribution to smaller sizes. The catalyst prepared under pH value of 10 exhibited the narrowest pore size distribution. The commercial catalyst exhibited broad pore size distribution in meso- and macro-regions, Fig. 1(a) (upper inset). The N_2 adsorption/desorption isotherms of the prepared catalysts are also shown in Fig. 1(b). The observed isotherms can be classified as type

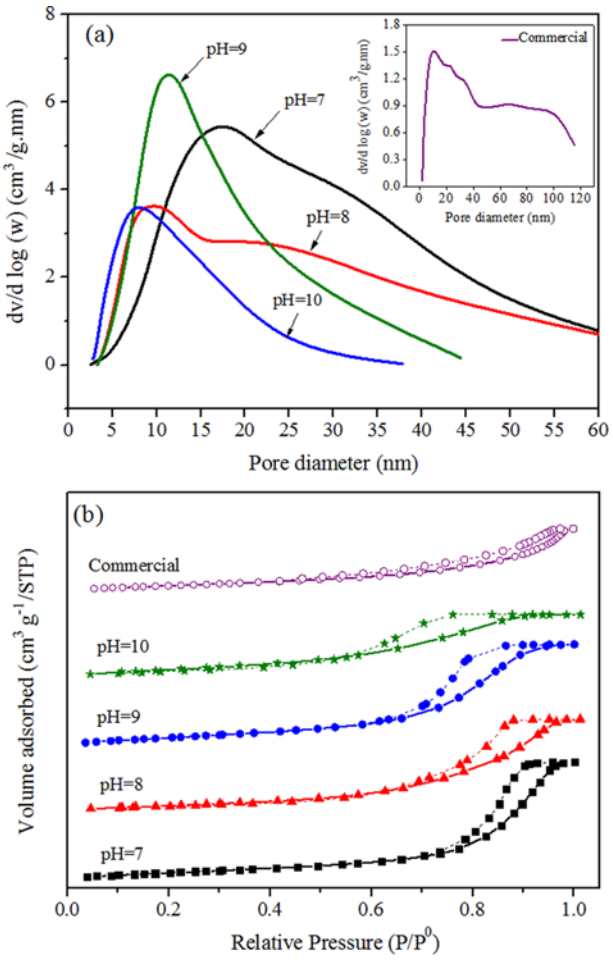

Fig. 1. (a) Pore size distributions and (b) N_2 adsorption/desorption isotherms of the catalysts prepared under different pH values, refluxing temperature=60 °C, refluxing time=5 h, concentration of the precursors solution=0.06 M and calcination temperature=400 °C.

IV isotherm, typical of mesoporous material. The shape of the curve indicates the absence of a narrow pore size distribution as suggested by the lack of the typical step in the adsorption isotherm, which is observed with ordered mesoporous structure. According to IUPAC classification, the hysteresis loop is of type H2 indicating complex mesoporous structure. The results clearly show that increasing in pH value shifted the hysteresis loop to lower relative pressures (p/p^0), implying a decrease of the pore diameter and a narrower pore size distribution for the samples prepared under higher pH values. The N_2 adsorption/desorption isotherm of the commercial catalyst can be classified as a type V isotherm with a H3-type hysteresis, which is usually attributed to large mesopores or macropores surrounded by a matrix of much smaller pores. For commercial catalyst formation of the hysteresis loop at high p/p^0 relative pressure confirmed the broad pore size distribution of this catalyst.

The structural properties of the prepared catalysts under different pH values are presented in Table 1. Increasing in pH value increased the BET surface area and decreased the average pore size. As can be seen, the sample prepared at pH value of 10 exhibited the highest surface area and the smallest pore size. The results show

Table 1. Structural properties of the prepared catalysts under different pH values

Catalyst	Surface area ($m^2\ g^{-1}$)	Pore volume ($cm^3\ g^{-1}$)	Pore size (nm)	Particle size* (nm)	Lattice parameter (A°)		
					a	b	c
pH=7	93.9	0.4	12.2	12.1	5.0023	5.0023	13.6246
pH=8	97.7	0.3	9.2	11.7	4.9832	4.9832	13.5754
pH=9	112.7	0.3	8.3	10.1	4.9753	4.9753	13.5471
pH=10	121.6	0.2	5.9	9.4	-	-	-
Commercial	76	0.2	10.4	15.0	-	-	-

Refluxing temperature=60 °C, refluxing time=5 h, concentration of the precursors solution=0.06 M and calcination temperature=400 °C
*Determined by BET area

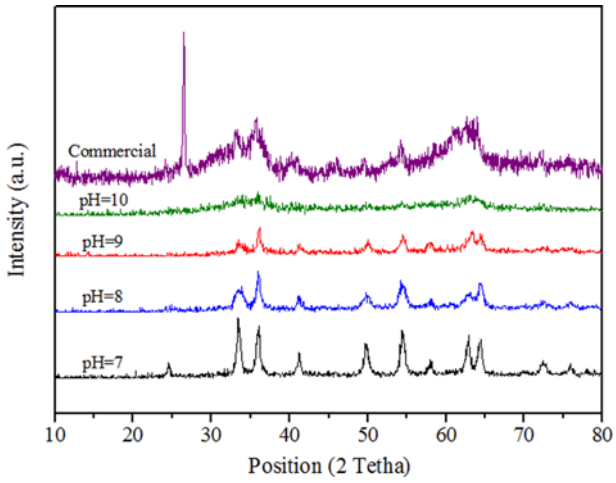

Fig. 2. XRD patterns of the catalysts prepared under different pH values, refluxing temperature=60 °C, refluxing time=5 h, concentration of the precursor solution=0.06 M and calcination temperature=400 °C.

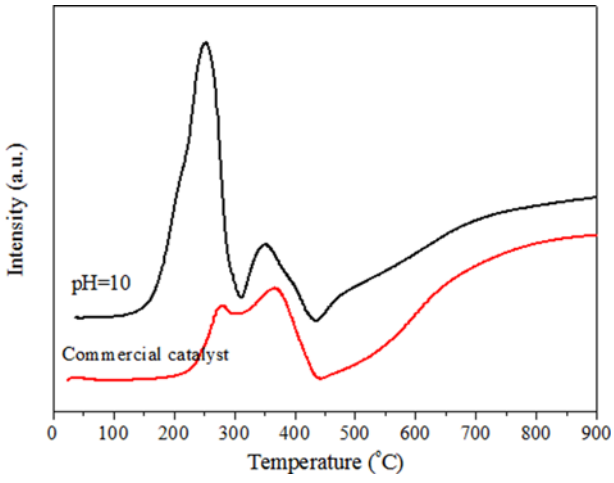

Fig. 3. TPR analysis of the prepared catalyst at pH value of 10 (refluxing temperature=60 °C, refluxing time=5 h, concentration of the precursor solution=0.06 M and calcination temperature=400 °C) and the commercial catalyst.

that all catalysts exhibited higher surface area and smaller particle size compared to commercial catalyst.

The XRD patterns of the catalysts prepared under different pH values are displayed in Fig. 2. α-Fe_2O_3 (α-Fe_2O_3, ICDD# 01-1053) was found in all the prepared catalysts and no crystalline phases related to Cr or Cu were observed. It is noted that CuO content in the prepared catalysts was lower than 3 wt%, which is difficult to detect by XRD analysis. In addition, the ionic radius of Cu^{2+} (0.73 Å) is similar to the Fe^{3+} (0.74 Å), which causes the incorporation of Cu^{2+} into the hematite lattice rather than to segregate as a separate crystalline phase.

Furthermore, the ionic radius of chromium is similar to Fe^{3+} and these two oxides could form a mixed oxide. In addition, the diffraction lines of this compound are in coincidence with those of iron oxide [12]. Both these reasons make it difficult to identify the iron chromium oxide species from hematite in XRD patterns. For the commercial catalyst the sharp diffraction peak at 28° is related to graphite, which is used during the shaping of catalyst powder.

The XRD analysis showed that increasing in pH value decreased the crystallinity of the prepared catalysts. Increasing in pH value decreased the peak intensities in XRD pattern, indicating a decrease in crystallite size of the catalysts prepared under higher pH values. As can be seen, the prepared catalyst at pH value of 10 exhibits a low degree of crystallinity. The degree of crystallinity is related to degree of supersaturation during the nucleation and crystal growth processes. The supersaturation degree is affected by temperature, pH value and reactant concentration. Increasing in pH value increased the supersaturation degree, which caused the formation of new nuclei at a faster rate than crystal growth. This difference between the rate of formation and crystal growth gives the product with lower crystallinity and particle size.

The lattice parameters (a, b and c) were obtained from the diffraction peaks at around 2θ=33° and 64° using the corresponding expression for hexagonal structure.

$$\frac{1}{d_{hkl}^2}=\frac{4}{3}\cdot\frac{(h^2+k^2+hk)}{a^2}+\frac{l^2}{c^2} \quad (1)$$

From the calculated lattice parameters presented in Table 1, increasing in pH value decreased the lattice constants. The decrease in lattice constants is accompanied with a decrease in the intensities of the XRD peaks (lowering the crystallite size), as shown in Table 1.

TPR results of the catalyst with the highest surface area (prepared at pH=10) and the commercial catalyst are shown in Fig. 3. For the prepared catalyst, three reduction peaks were observed in TPR profile. The lower temperature peak observed at 240 °C is related to the reduction of CuO to metallic copper and CrO_3 to Cr_2O_3. The

second reduction peak at 350 °C is assigned to the reduction of Fe_2O_3 to Fe_3O_4 and the last broad peak is due to reduction of Fe_3O_4 to FeO and metallic iron. The commercial catalyst also exhibited a similar TPR profile with three reduction peaks. The T_{max} of the first and the second reduction peaks in commercial catalyst are shifted to higher temperatures, indicating the lower reducibility of the commercial catalyst compared to the prepared catalyst in this work.

The catalytic results of the catalysts prepared under different pH values are presented in Fig. 4. Increasing in reaction temperature increased the CO conversion, except of the catalyst prepared under the pH value of 10. The conversion of this catalyst decreased with increasing the reaction temperature higher than 450 °C. The obtained results showed that increasing in pH value improved the CO conversion, due to improvement in BET surface area (Table 1).

The effect of refluxing temperature on the XRD patterns of the prepared catalysts is shown in Fig. 5. The results confirm the existence of α-Fe_2O_3 phase in all samples. In addition, no phases related to Cr or Cu species were observed. Increasing in refluxing temperature decreased the degree of crystallinity. The textural properties of the prepared samples under different refluxing temperatures are presented in Table 2. The results show an increase in the specific surface area and a decrease in particle size with increasing in refluxing temperature. This increase in surface area is more obvious from 40 to 60 °C. Increasing the refluxing temperature higher

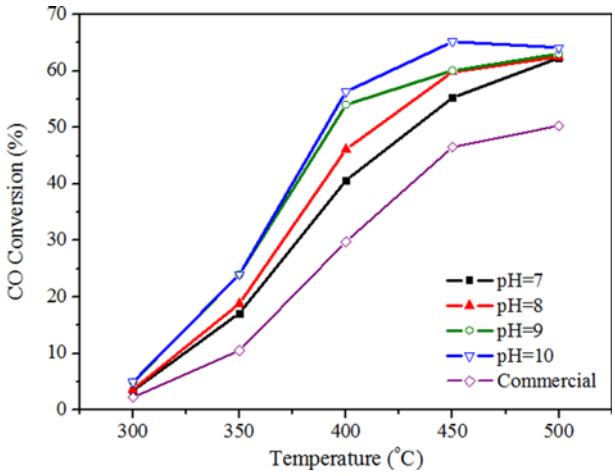

Fig. 4. CO conversion of the catalysts prepared at different pH values and calcined at 400 °C, GHSV=3×10⁴ mL/h·g_{cat}, and steam/gas=0.6.

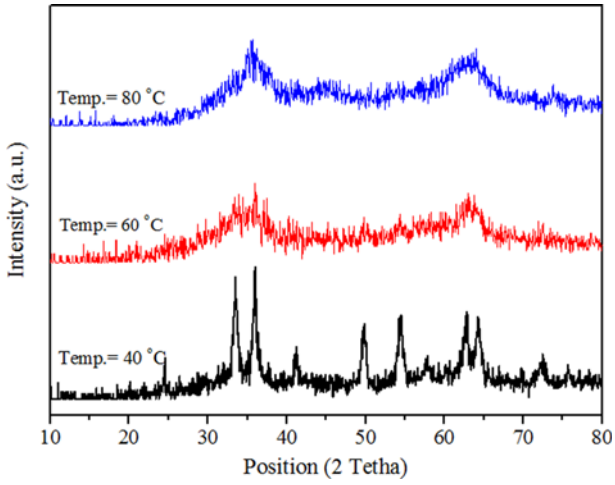

Fig. 5. XRD patterns of the catalysts prepared under different refluxing temperatures, pH=10, aging time=5 h, concentration of the precursor solution=0.06 M and calcination temperature =400 °C.

Table 2. Structural properties of the prepared catalysts under different refluxing temperatures

Refluxing temperature (°C)	Surface area ($m^2\ g^{-1}$)	Pore volume ($cm^3\ g^{-1}$)	Pore size (nm)	Particle size* (nm)
40	96.0	0.3	8.5	11.9
60	121.6	0.2	5.9	9.4
80	122.2	0.4	8.4	9.3

Refluxing time=5 h, pH=10, concentration of the precursors solution =0.06 M and calcination temperature=400 °C
*Determined by BET area

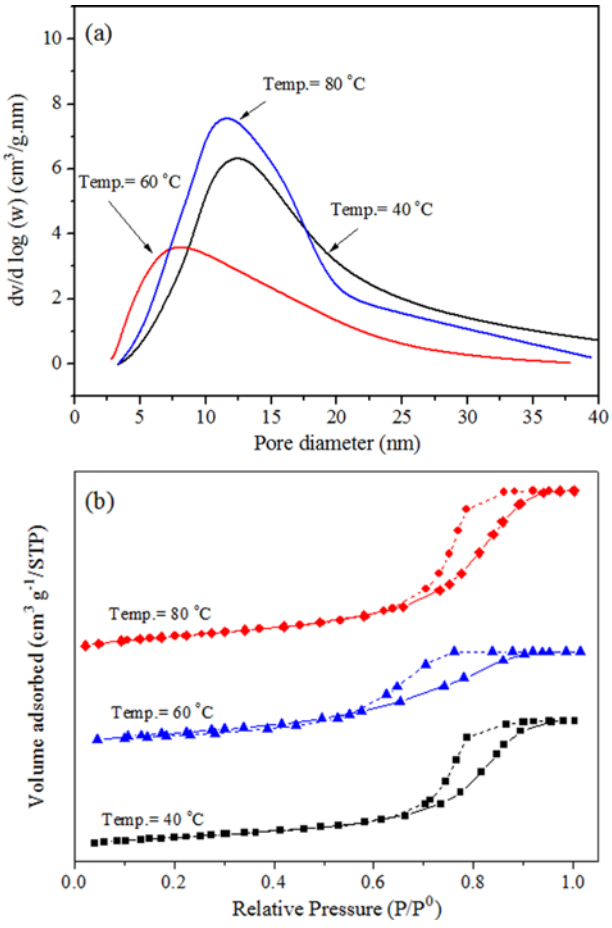

Fig. 6. (a) Pore size distributions and (b) N_2 adsorption/desorption isotherms of the catalysts prepared under different refluxing temperatures, pH=10, aging time=5 h, concentration of the precursor solution=0.06 M and calcination temperature= 400 °C.

than 60 °C did not have a significant effect on the BET surface area.

The pore size distributions of the catalysts prepared under different refluxing temperatures are shown in Fig. 6. All samples exhibit a single modal pore size distribution. As can be seen, increasing in refluxing temperature shifted the pore size distributions to smaller sizes. Among the prepared catalysts, the sample prepared at refluxing temperature of 60 °C exhibited the pore size distribution in smaller region. The N_2 adsorption/desorption of the catalysts prepared at different refluxing temperatures also shows a type IV isotherm with the H2 hysteresis loop.

The catalytic results of the samples prepared at different refluxing temperatures are shown in Fig. 7. CO conversion improved by increasing refluxing temperature from 40 °C to 60 °C, but further increase of temperature did not have a significant effect on the CO conversion. Both catalysts prepared under refluxing temperature of 60 and 80 °C possessed a similar BET surface area (Table 2) and consequently a similar catalytic activity.

Fig. 8 shows the XRD patterns of the catalysts prepared under different refluxing times. With increasing in refluxing time, the intensities of the peaks decreased, which indicates the lower crystallinity (lower crystallite size) of the samples prepared under higher refluxing times. The sample prepared under refluxing time of 5 h exhibited the lowest degree of crystallinity. The sample prepared under refluxing time of 10 h exhibited higher crystallinity compared to

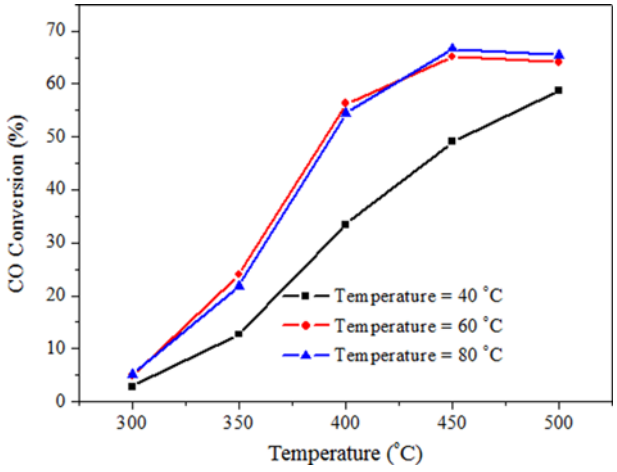

Fig. 7. CO conversion of the catalysts prepared under different refluxing temperatures and calcined at 400 °C, GHSV=3×10^4 mL/h·g_{cat} and steam/gas=0.6.

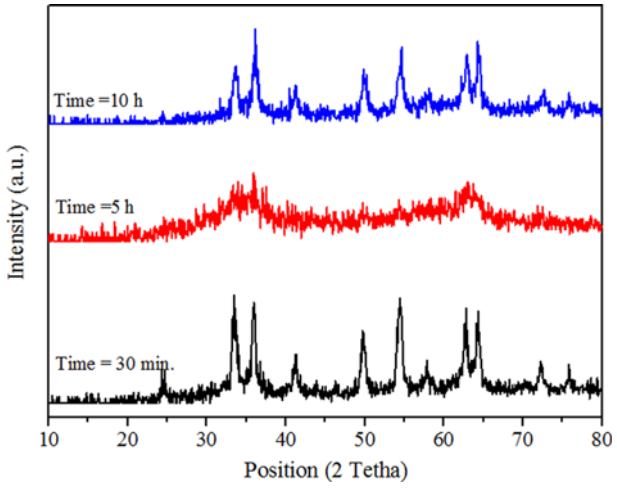

Fig. 8. XRD patterns of the catalysts prepared under different refluxing times, pH=10, aging temperature=60 °C, concentration of the precursor solution=0.06 M and calcination temperature=400 °C.

Table 3. Structural properties of the prepared catalysts under different refluxing times

Refluxing time	Surface area (m^2 g^{-1})	Pore volume (cm^3 g^{-1})	Pore size (nm)	Particle size* (nm)
30 min	84.7	0.3	9.1	13.4
5 h	121.6	0.2	5.9	9.4
10 h	103.4	0.2	6.3	11.0

Refluxing temperature=60 °C, pH=10, concentration of the precursors solution=0.06 M and calcination temperature=400 °C
*Determined by BET area

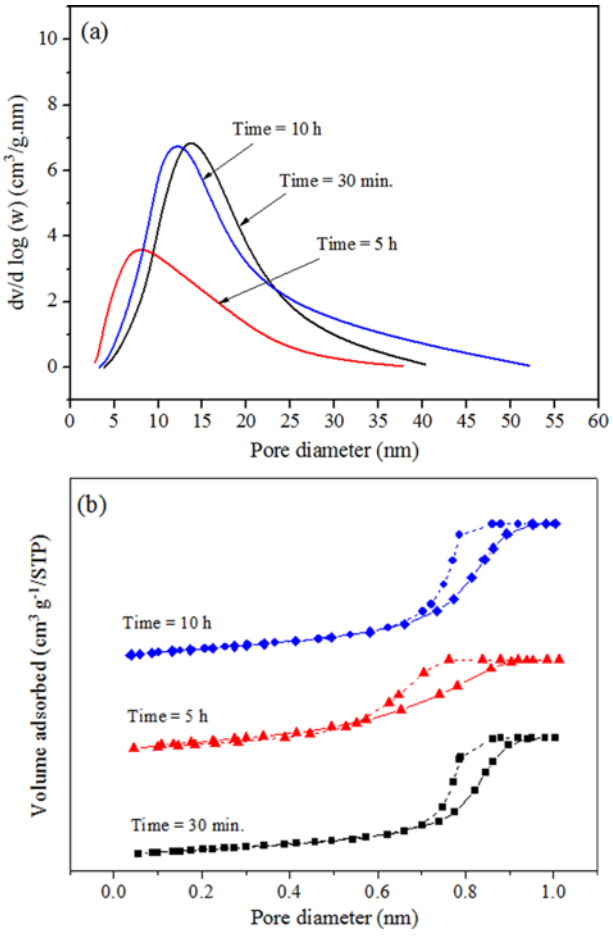

Fig. 9. (a) Pore size distributions and (b) N_2 adsorption/desorption isotherms of the catalysts prepared under different refluxing temperatures, pH=10, refluxing temperature=60 °C, concentration of the precursor solution=0.06 M and calcination temperature=400 °C.

the sample prepared under refluxing time of 5 h. This might be due to more time for growth of nuclei.

The structural properties of the prepared catalysts under different refluxing times are presented in Table 3. The surface area increased and the pore size decreased by increasing in refluxing time up to 5 h. Further increase in refluxing time decreased the BET surface area and increased the pore and particle sizes.

The pore size distributions of the prepared catalysts under different refluxing times are shown in Fig. 9(a). Increasing in refluxing time shifted the pore size distribution to smaller sizes. The catalyst prepared under refluxing time of 5 h exhibits the smallest pore size distribution. The N_2 adsorption/desorption isotherm of these samples are presented in Fig. 9(b). All samples show a type IV isotherm, with the H2 hysteresis loop. The hysteresis loop of the sample prepared under refluxing time of 5 h was observed at lower relative pressure, which confirms the formation of smaller mesopores (Fig. 9(a)).

Fig. 10 shows the CO conversion of the catalysts prepared under different refluxing times. The results show that increasing in refluxing time from 30 min to 5 h increased the CO conversion. But further increase in refluxing time did not have a positive effect on the CO conversion. The catalyst prepared under 5 h refluxing time exhibits the highest catalytic activity among the prepared catalysts. It is

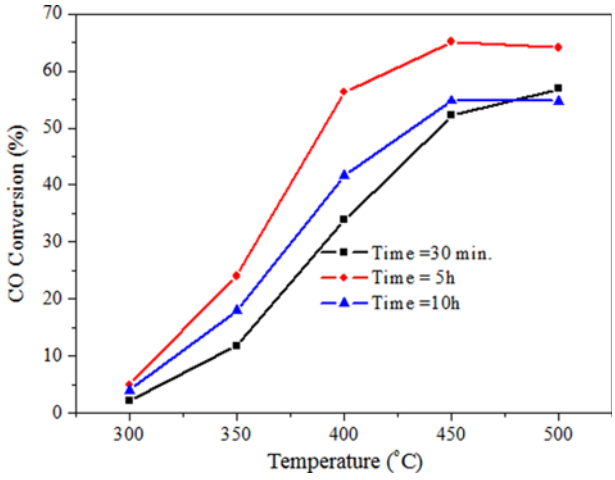

Fig. 10. CO conversion of the catalysts prepared under different refluxing times and calcined at 400 °C, GHSV=3×10^4 mL/h·g_{cat} and steam/gas=0.6.

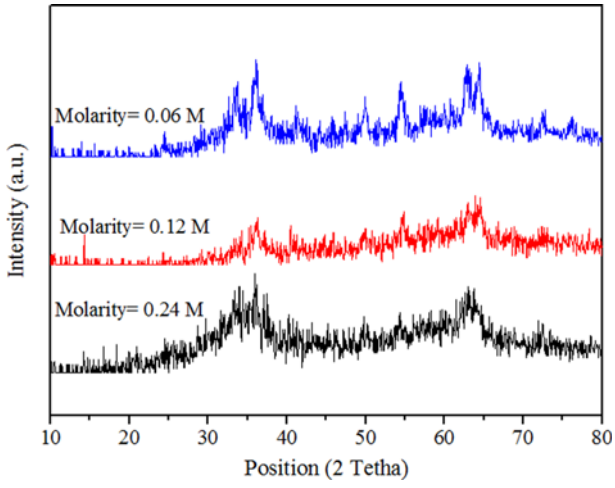

Fig. 11. XRD patterns of the catalysts prepared with different precursor solution concentrations, pH=10, refluxing time=5 h, refluxing temperature=60 °C and calcination temperature=400 °C.

Table 4. Structural properties of the catalysts prepared with different precursor solution concentrations

Precursor concentration	Surface area (m^2 g^{-1})	Pore volume (cm^3 g^{-1})	Pore size (nm)	Particle size* (nm)
Molarity=0.06 mol/lit	121.6	0.2	5.9	9.4
Molarity=0.12 mol/lit	128.7	0.4	8.3	8.9
Molarity=0.24 mol/lit	123.7	0.3	7.5	9.2

Refluxing temperature=60 °C, refluxing time=5 h, pH=10 and calcination temperature=400 °C

*Determined by BET area

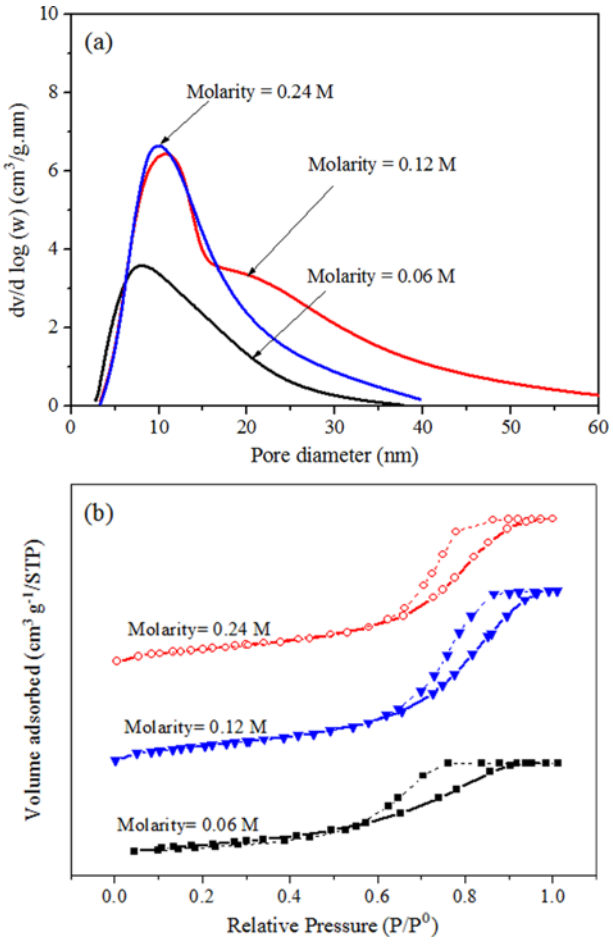

Fig. 12. (a) Pore size distributions and (b) N_2 adsorption/desorption isotherms of the catalysts prepared under different precursor solution concentrations, pH=10, refluxing time=5 h, refluxing temperature=60 °C and calcination temperature=400 °C.

notable that the catalyst prepared under 5 h refluxing time has the highest BET surface area and consequently the highest CO conversion.

Fig. 11 shows the XRD patterns of the samples prepared under different precursor solution concentrations. All catalysts exhibit a low degree of crystallinity. However, the sample prepared with a precursor solution concentration of 0.06 M shows the highest degree of crystallinity.

The structural properties of the prepared catalysts with different precursor solution concentrations are presented in Table 4. The results show that increasing in precursor solution concentration did not have a significant effect on the BET surface area. However, the catalyst prepared with a molarity of 0.12 mol/lit exhibits the highest BET area and the smallest particle size.

The pore size distributions of these catalysts are shown in Fig. 12(a). All catalysts exhibit a broad pore size distribution. The catalyst prepared with a precursor solution concentration of 0.12 exhibits the broadest pore size distribution.

The N_2 adsorption/desorption isotherms of the prepared catalysts with different precursor solution concentrations exhibited type IV isotherm with the H2 hysteresis loop (Fig. 12(b)). The precursor solution concentration does not have a significant effect on the N_2 adsorption/desorption profiles.

The effect of precursor solution concentration on the catalytic activity is shown in Fig. 13. The results show that the decrease in precursor solution concentration improved the CO conversion and

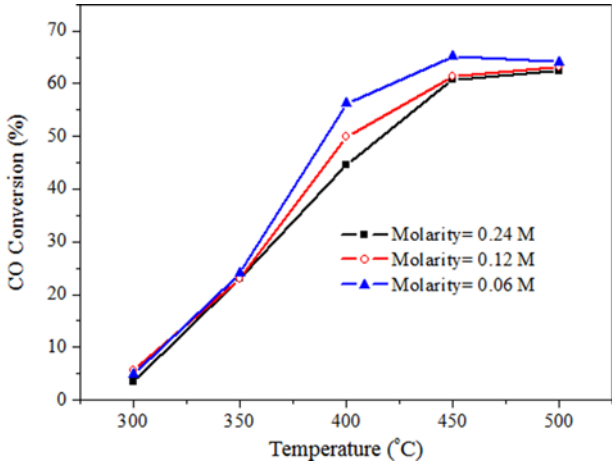

Fig. 13. CO conversion of the catalysts prepared under different precursor solution concentrations and calcined at 400 °C, GHSV=3×10^4 mL/h·g_{cat} and steam/gas=0.6.

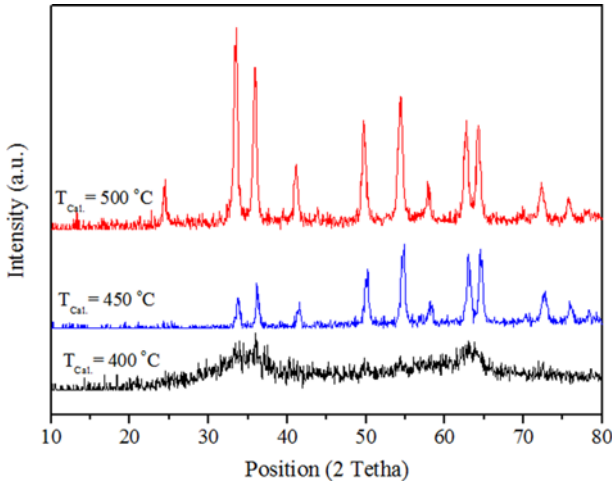

Fig. 14. XRD patterns of the catalysts calcined at different temperatures, refluxing temperature=60 °C, refluxing time=5 h, pH=10, concentration of the precursor solution=0.06 M.

Table 5. Structural properties of the prepared catalysts calcined at different temperatures

Temperature (°C)	Surface area (m^2 g^{-1})	Pore volume (cm^3 g^{-1})	Pore size (nm)	Particle size* (nm)
400	121.6	0.2	5.9	9.4
450	52.0	0.3	13.9	21.9
500	25.9	0.3	23.4	44.0

Refluxing temperature=60 °C, refluxing time=5 h, pH=10, concentration of the precursors solution=0.06 M
*Determined by BET area

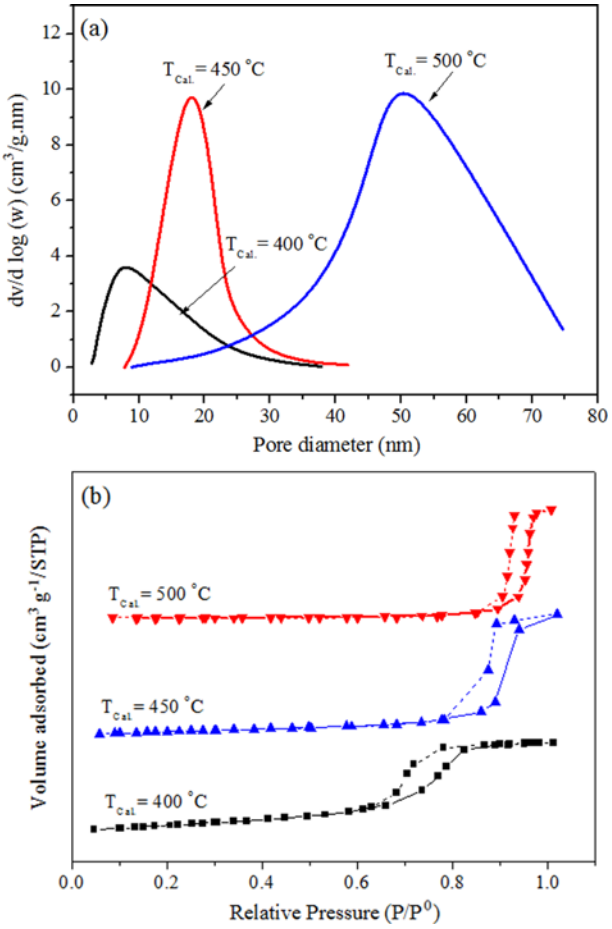

Fig. 15. (a) Pore size distributions and (b) N_2 adsorption/desorption isotherms of the samples calcined at different temperatures, refluxing temperature=60 °C, refluxing time=5 h, pH=10, concentration of the precursor solution=0.06 M.

the catalyst prepared with the lowest concentration of the precursor solution presented the highest activity.

The XRD patterns of the catalysts calcined at different temperatures are shown in Fig. 14. Increasing in calcination temperature increased the degree of crystallinity and the peak intensities due to growth of crystals and construction to lager clusters. The particle size increases with increasing the calcination temperature, Table 5.

The effect of calcination temperature on the structural properties of the catalyst with the highest activity is presnted in Table 5. The BET surface area decreased with increasing in calcination temperature due to growth of crystals, Fig. 14. In addition, increasing in calcination temperature shifted the pore size to bigger sizes, Table 5.

The pore size distributions and N_2 adsorption/desorption isotherms of the catalysts calcined at different temperatures are shown in Fig. 15(a) and 15(b), respectively. The results show that increasing in calcination temperature shifted the pore size distribution to larger sizes (Fig. 15(a)). Increasing in calcination temperature shifted the hysteresis loop of the calcined catalysts to higher relative pressures, indicating larger pores (Fig. 15(b)). In addition, the type of hysteresis loop changed from the H2 type for the catalyst calcined at 400 °C to H1 type for the catalysts calcined at 450 and 500 °C, which is characteristic of solids consisting of particles crossed by nearly cylindrical channels or made by aggregates (consolidated) or agglomerates (unconsolidated) of spheroidal particles. In this case the pores can have uniform size and shape.

The TPR profiles of the catalysts calcined at different temperatures are shown in Fig. 16. The calcination temperature does not have a significant effect on the reducibility of the calcined catalysts. Increasing in calcination temperature shifted the T_{max} of reduction of Fe_2O_3 to Fe_3O_4 to higher temperatures and reduced the reduc-

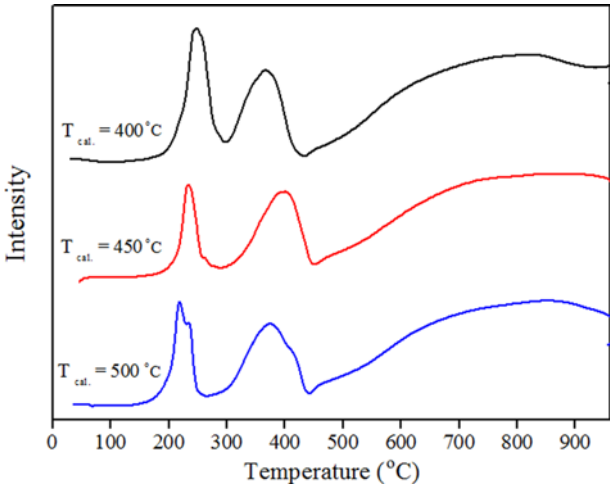

Fig. 16. TPR analysis of the calcined catalysts at different temperatures, refluxing temperature=60 °C, refluxing time=5 h, pH=10, concentration of the precursor solution=0.06 M.

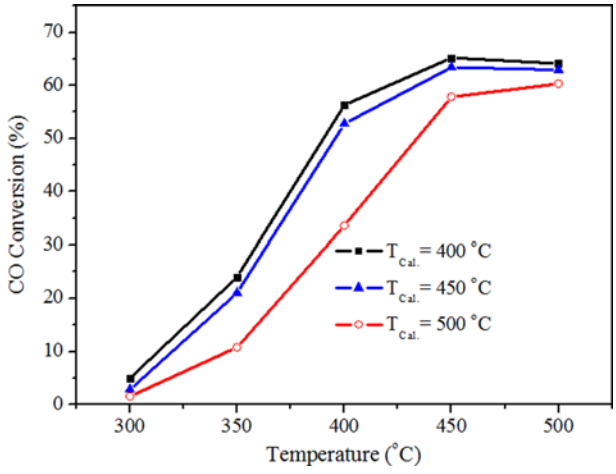

Fig. 17. CO conversion of the catalysts calcined at different temperatures, GHSV=3×10^4 mL/h·g_{cat}, and steam/gas=0.6.

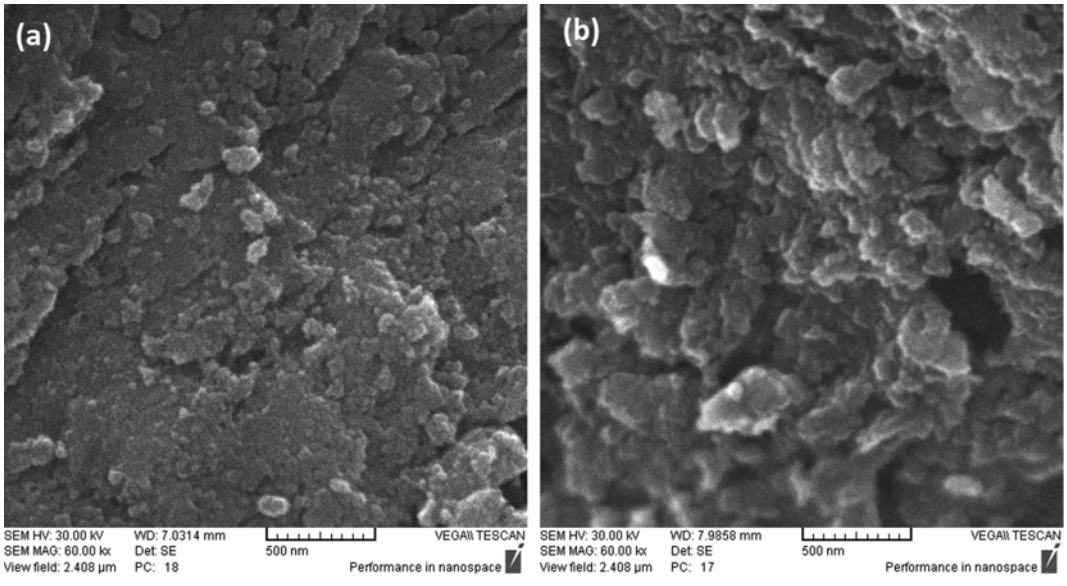

Fig. 18. SEM analysis of the catalysts calcined at (a) 400 °C and (b) 500 °C, refluxing temperature=60 °C, refluxing time=5 h, pH=10, concentration of the precursor solution=0.06 M.

ibility of the catalyst.

Fig. 17 shows the CO conversion of the catalysts calcined at different temperatures. The results show that increasing in calcination temperature decreased the catalytic activity due to loss of surface area caused by sintering at high temperatures. In other word, as illustrated in Table 5, when the calcination temperature increased, the surface particles were highly agglomerated and led to increase in the particle and decrease in the specific surface area.

The SEM images of the catalysts calcined at different temperatures are shown in Fig. 18. The SEM analysis clearly shows an increase in the particle size of the catalyst calcined at 500 °C, due to agglomeration of particles at higher temperatures.

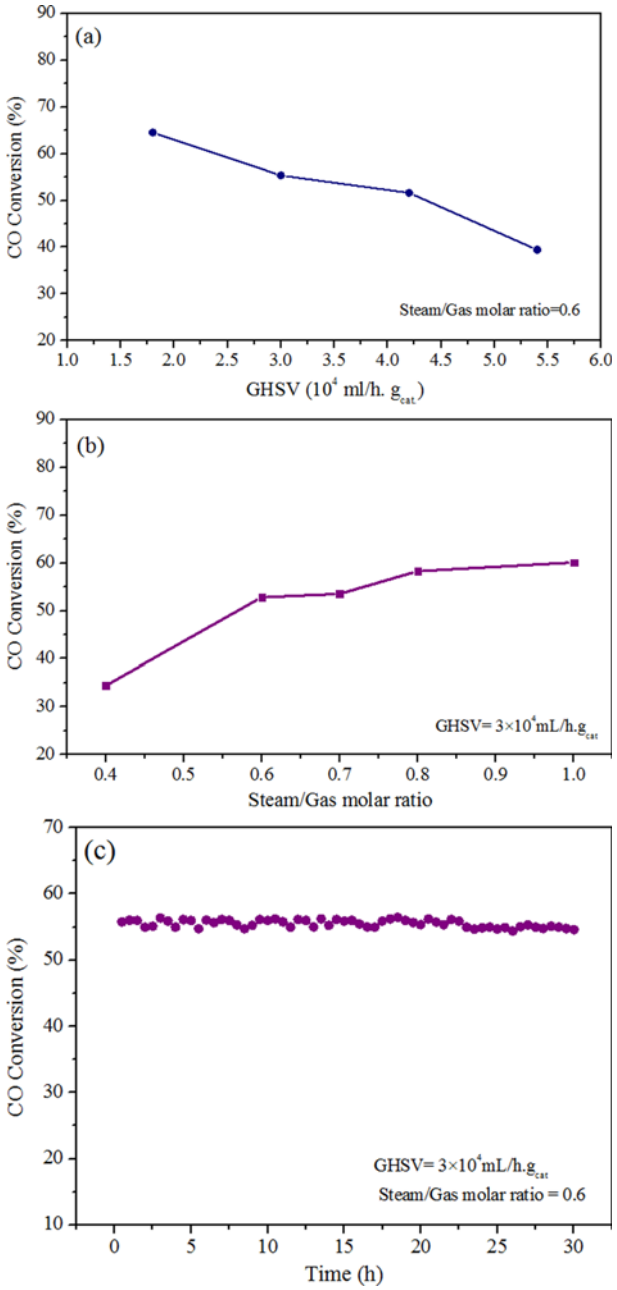

Fig. 19. Effect of (a) GHSV and (b) steam/dry gas molar ratio and (c) time on stream (stability test) on CO conversion at 400 °C, refluxing temperature=60 °C, refluxing time=5 h, pH=10, concentration of the precursor solution=0.06 M and calcination temperature=400 °C.

The effects of GHSV and steam/gas molar ratio on the CO conversion of the catalyst with the highest activity are shown in Fig. 19(a) and 19(b), respectively. Increasing GHSV decreased the catalytic activity due to decreasing the contact time (Fig. 19(a)). In addition, increasing the molar steam to dry gas ratio (S/G) increased the CO conversion due to favorable effect on the equilibrium of high concentrations of water (Fig. 19(b)). In addition, the results show a high stability without any decrease in CO conversion for the prepared catalyst with the highest activity (Fig. 19(c)).

The structural properties of the fresh and spent catalysts tested at 400 °C for 100 h under the reaction condition of GHSV=3×10^4 mL/h·g_{cat}, and steam/gas=0.6 are presented in Table 6. The BET surface area of the spent catalyst was lower than that of the fresh catalyst. In addition, the spent catalyst exhibits lower pore volume and bigger pore size compared to that observed for the fresh catalyst. Fig. 20 shows the pore size distributions and N_2 adsorption/desorption isotherms (upper inset) of the fresh and spent catalysts. The fresh catalyst exhibits a narrower pore size distribution centered at 8 nm. After the reaction the pore size distribution of the catalyst shifted towards bigger sizes (12 nm) and this catalyst exhib-

Table 6. Structural properties of the fresh and spent Fe-Cr-Cu catalysts, refluxing temperature=60 °C, refluxing time=5 h, pH=10, concentration of the precursors solution=0.06 M

Catalyst	Surface area (m^2 g^{-1})	Pore volume (cm^3 g^{-1})	Pore size (nm)	Particle size (nm)*
Fresh	121.6	0.2	5.9	9.4
Spent	25.0	0.1	10.3	45.6

*Determined by BET area

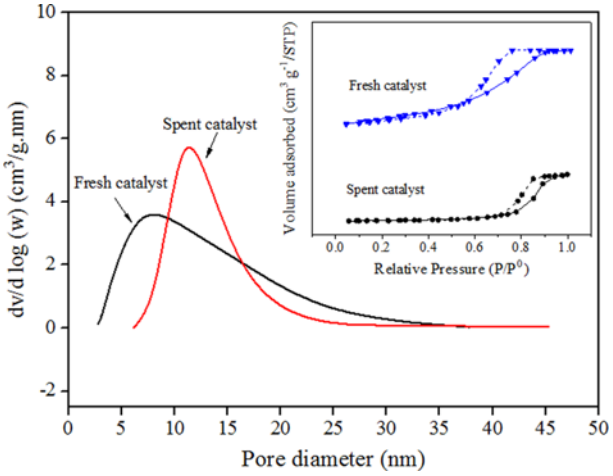

Fig. 20. Pore size distributions and N_2 adsorption/desorption isotherms (upper inset) of the fresh and spent catalysts, refluxing temperature=60 °C, refluxing time=5 h, pH=10, concentration of the precursor solution=0.06 M and calcination temperature=400 °C, reaction condition of spent catalyst: 100 h time on stream at 400 °C, GHSV=3×10^4 mL/h·g_{cat}, and steam/gas=0.6.

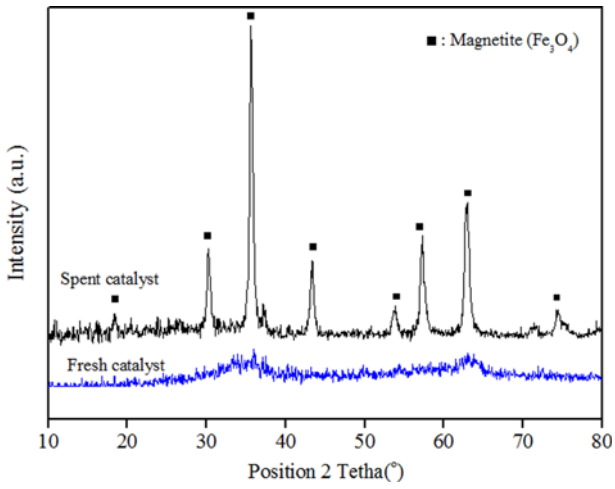

Fig. 21. XRD analysis of the fresh and spent catalysts, refluxing temperature=60 °C, refluxing time=5 h, pH=10, concentration of the precursor solution=0.06 M and calcination temperature=400 °C. Reaction condition of spent catalyst: 100 h time on stream at 400 °C, GHSV=3×10^4 mL/h·g_{cat}, and steam/gas=0.6.

ited a broader pore size distribution, indicating a lower surface area compared to the fresh catalyst. In addition, both the fresh and spent catalysts exhibit type IV isotherm with an H2-type hysteresis loop (upper inset). For the spent catalyst, the hysteresis loop occurred at higher relative pressure confirming a broader pore size distribution of the spent catalyst compared to the fresh one. For the fresh catalyst the hysteresis loop formed at a lower p/p^0 relative pressure, indicating a narrower pore size distribution (Fig. 20).

Fig. 21 shows the XRD patterns of the fresh and spent catalysts. The fresh catalyst exhibits a low degree of crystallinity. However, the spent catalyst shows a high degree of crystallinity and all the

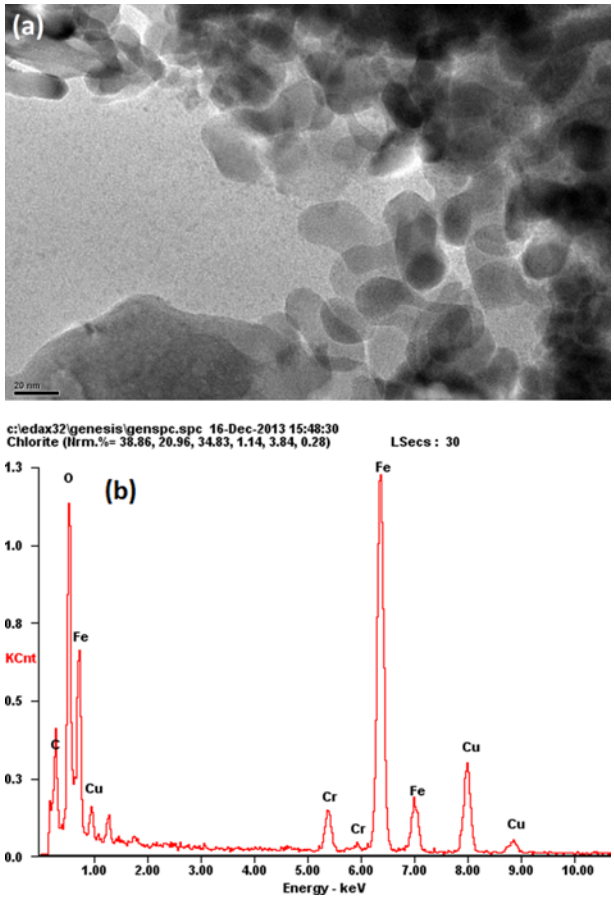

Fig. 23. (a) TEM and (b) EDX analysis of the fresh catalyst.

diffraction peaks in XRD patterns of the spent catalyst can be indexed to the phase of Fe_3O_4, an active phase for HTS reaction. In addition, the diffraction peaks in the spent catalyst show higher inten-

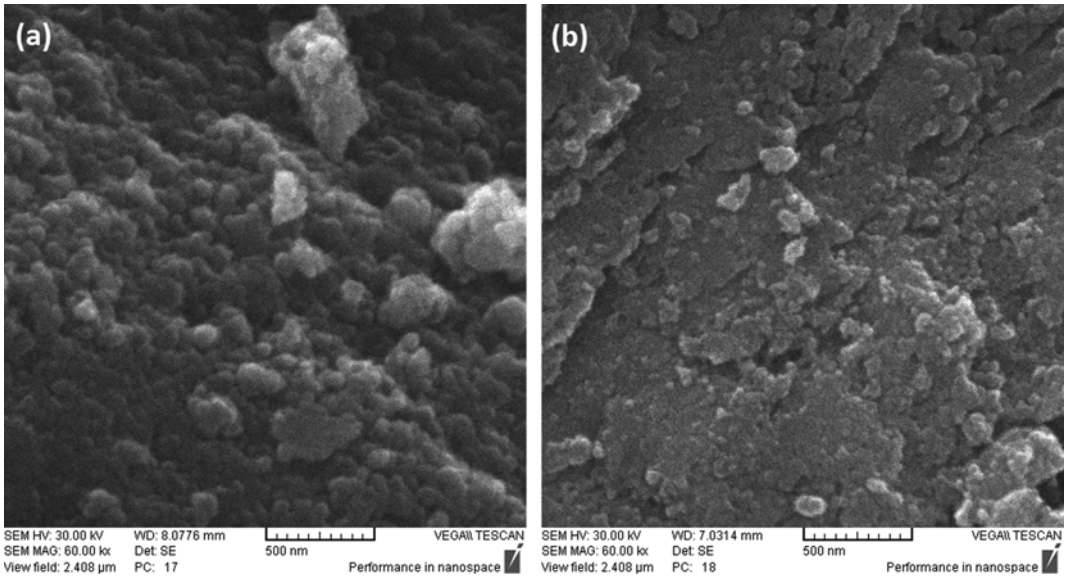

Fig. 22. SEM analysis of (a) spent and (b) fresh catalyst, reaction condition of spent catalyst: 100 h time on stream at 400 °C, GHSV=3×10^4 mL/h·g_{cat}, and steam/gas=0.6.

sities compared to those observed for the fresh catalyst, indicating the bigger crystallite size of the spent catalyst.

The SEM images of the spent and fresh catalysts are shown in Fig. 22(a) and 22(b), respectively. The fresh catalyst exhibits the particle sizes in nano scale. In the spent catalyst the particles are sintered together and form bigger particles. These results are in agreement with the particle sizes calculated from the BET area (Table 6), which show bigger particle size for the spent catalyst compared to the fresh one.

In addition, the TEM analysis (Fig. 23(a)) of the fresh catalyst reveals that the crystals are in nanometer scale with a particle size less than 20 nm. The EDX analysis (Fig. 23(b)) shows the presence of Fe, Cr and Cu elements in this catalyst.

CONCLUSIONS

A systematic study was done on the effect of preparation factors on the structural and catalytic properties of mesoporous nanocrystalline iron-based catalysts in high temperature water gas shift reaction. The obtained results show that in coprecipitation method thte increasing in pH value increased the BET surface area and improved the catalytic activity. The increase in pH value decreased the lattice constants, which is accompanied with decrease in crystallite size. In addition, increasing in refluxing temperature up to 60 °C increased the BET surface area and catalytic activity, but further increase in refluxing temperature did not have a significant effect on the BET surface area and catalytic properties. There was an optimum for refluxing time and the catalyst prepared with refluxing time of 5 h exhibited the highest surface area and catalytic activity. Moreover, decreasing in calcination temperature had a positive effect on the catalytic activity. The TEM analysis shows a nanostructure (with particle size less than 20 nm) for the fresh catalyst with the highest activity. The results reveal that in the spent catalyst the particles were sintered together and formed bigger particles.

ACKNOWLEDGEMENT

The authors are grateful to University of Kashan for supporting this work by Grant No. 158426/47.

REFERENCES

1. G. Ertl, H. Knozinger and J. Weitkamp, Handbook of Heterogeneous Catalysis, Vol. 4. Weinheim, Wiley-VCH (1997).
2. Y. Lei, N. W. Cant and D. L. Trimm, *J. Catal.*, **239**, 227 (2006).
3. F. Meshkani and M. Rezaei, *J. Ind. Eng. Chem.*, **20**, 3297 (2014).
4. G. Jacobs, S. Ricote and B. H. Davis, *Appl. Catal. A.*, **302**, 14 (2006).
6. (1) H. Yahiro, K. Murawaki, K. Saiki, T. Yamamoto and H. Yamaura, *Catal. Today*, **126**, 436 (2007).
   (2) V. Galvita and K. Sundmacher, *Chem. Eng. J.*, **134**, 168 (2007).
7. L. Loyd, D. E. Ridler and M. V. Twigg, Catalysis Handbook, Wolfe Scientific Books (1996).
8. V. Idakiev, A. D. Mihajlo, B. Kanev and A. Andreev, *React. Kinet. Catal. Lett.*, **33**, 119 (1987).
9. A. Andreev, V. Idakiev, D. Mihajlova and D. Shopov, *Appl. Catal.*, **22**, 385 (1986).
10. E. Matijevic and P. Sheider, *J. Colloid Interface Sci.*, **63**, 509 (1978).
11. M. S. Santos, A. Albornoz and M. C. Rangel, *Stud. Surf. Sci. Catal.*, **162**, 753 (2006).
12. J. E. Huheey, E. A. Keiter and R. L. Keiter, *Inorganic Chemistry: Principles of Structure and Reactivity*, 4th Ed., Harper Collins, New York, NY (1993).